

Deep Generative Model for Periodic Graphs

Shiyu Wang¹ Xiaojie Guo² Liang Zhao³

Abstract

Periodic graphs are graphs consisting of repetitive local structures, such as crystal nets and polygon mesh. Their generative modeling has great potential in real-world applications such as material design and graphics synthesis. Classical models either rely on domain-specific predefined generation principles (e.g., in crystal net design), or follow geometry-based prescribed rules. Recently, deep generative models have shown great promise in automatically generating general graphs. However, their advancement into periodic graphs have not been well explored due to several key challenges in 1) maintaining graph periodicity; 2) disentangling local and global patterns; and 3) efficiency in learning repetitive patterns. To address them, this paper proposes Periodical-Graph Disentangled Variational Auto-encoder (PGD-VAE), a new deep generative models for periodic graphs that can automatically learn, disentangle, and generate local and global graph patterns. Specifically, we develop a new periodic graph encoder consisting of global-pattern encoder and local-pattern encoder that ensures to disentangle the representation into global and local semantics. We then propose a new periodic graph decoder consisting of local structure decoder, neighborhood decoder, and global structure decoder, as well as the assembler of their outputs that guarantees periodicity. Moreover, we design a new model learning objective that helps ensure the invariance of local-semantic representations for the graphs with the same local structure. Comprehensive experimental evaluations have been conducted to demonstrate the effectiveness of the proposed method. The code of proposed PGD-VAE is available at <https://github.com/shi-yu-wang/PGD-VAE>.

¹Department of Biostatistics and Bioinformatics, Emory University, Atlanta, USA ²JD.COM Silicon Valley Research Center, Mountain View, USA ³Department of Computer Science, Emory University, USA. Correspondence to: Shiyu Wang <shiyu.wang@emory.edu>, Liang Zhao <liang.zhao@emory.edu>.

1. Introduction

Graphs serve as a ubiquitous data structure that describes objects and their relations. As a special type of graphs, periodic graphs are graphs that consist of repetitive local structures. They naturally characterize many real-world applications ranging from crystal nets containing repetitive unit cells to polygon mesh data containing repetitive grids (Figure 1). Hence, understanding, modeling, and generating periodic graphs have great potential in real-world applications such as material design and graphics synthesis. Different from general graphs, modeling generative process of periodic graphs requires to ensure the periodicity. Therefore, conventional graph models such as random graphs, small-world models, etc. cannot be used effectively. The classical studies on periodic graph generative models have a long history, where the conventional methods can be categorized into two types: domain specific-based and geometry-based. Specifically, domain specific-based models generate periodic graphs relying on the properties hand-crafted based on domain knowledge (Xie et al., 2021; Bushlanov et al., 2019). In addition, geometry-based methods generate periodic graphs either according to predefined geometric rules to craft the targeted periodic graphs (Friedrichs et al., 1999; Treacy et al., 2004) or simply gluing the initial fragment into periodic graphs (Le Bail, 2005).

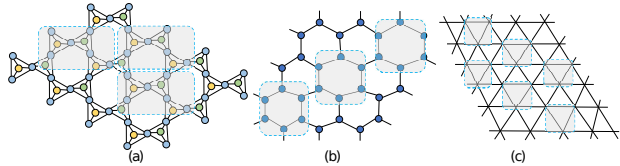


Figure 1. Examples of periodic graphs where basic units are highlighted: (a) structure of tridymite; (b) structure of graphene and (c) triangular grids (Korn & Linardakis, 2018)

As mentioned above, both domain specific-based and geometry-based generative models for periodic graphs require predefined properties that are either domain-specific or geometric-based, enabling them to usually fit well towards the properties that the predefined principles are tailored for, but usually they cannot do well for the others. For example, a geometry-based generative model can generate graphs within the predefined geometric rules but can-

not generalize to other geometric properties. However, in many domains, the network properties and generation principles are largely unknown, such as those for explaining the thermal probability (Tabero et al., 2018) and solubilities (Fan et al., 2019a) of materials. Here the lack of predefined principles leads to the incapability of existing methods to model periodic graphs. Hence, it is imperative to fill the gap between the lack of powerful models and the complex generative process of periodic graphs.

Expressive generative models that can directly learn the underlying data generative process automatically have been an extremely challenging task to accomplish, until very recent years when the advancement of deep generative models have exhibited great success in data such as images and graphs (Ranzato et al., 2011; Guo & Zhao, 2020). Under this area, deep graph generative models aim at learning the distributions of general graph data representation extracted by graph neural networks. However, despite the progress in graph neural networks for general graphs, they cannot be directly applied to handle periodic graphs due to the additional requirements of the generated graphs such as periodicity. It requires significant efforts to advance the current deep graph generative models in order to handle periodic graphs due to the following unique challenges: (1) Difficulty in ensuring the periodicity of the generated graphs. Existing works for generic graph generative models typically are not able to identify or generate the “basic unit”, namely the repetitive local subgraphs. The conventional learning objective such as reconstruction errors or adversarial errors can only measure the generated graph quality globally but cannot ensure the identity of local structures as well as the how different local structures are connected. (2) How to jointly learn local and global topological patterns. In periodic graph, there are two key patterns, namely the local structure which specifies the basic unit and the global topology which characterizes how local structures are connected to form the whole graph topology. Therefore, it is imperative for the generative models to be able to factorize these two different patterns for respective characterization and control. However, Existing works for general graphs only learn a representation for the graph instead of disentangling them into different representations for local and global patterns; and (3) Efficiency in learning large periodic graphs. Due to the ubiquitousness of repetitive structures, periodic graphs are full of redundant information which makes existing works for generic graphs highly inefficient to model them. It is imperative to establish models that can automatically deduplicate the modeled generative process of periodic graphs.

To address these challenges, we developed Periodic-Graph Disentangled Variational Auto-encoder (PGD-VAE), a deep generative model for periodic graphs that can automatically learn, disentangle and generate local and global

graph patterns. Specially, we proposed a novel encoder that contains a local-pattern encoder and a global-pattern encoder to disentangle the local and global semantics from the periodic graph representation. Besides, we designed a periodic graph decoder consisting of a local structure decoder, a global structure decoder, a neighborhood decoder and an assembler to assemble local and global patterns while preserving periodicity. To achieve the disentanglement of local and global semantics, we proposed a new learning objective that can simultaneously ensure the invariance of the local-semantic representations of graphs that have the same basic unit. Our contributions can be summarized as follows:

- We propose a new problem of end-to-end periodic graph generative models by deep generative models.
- We develop PGD-VAE, a novel variational autoencoder that can decompose and assemble periodic graphs with the learned patterns of basic units, their pairwise relations, and their local neighborhoods.
- We propose a new learning objective to achieve the disentanglement of the local and global semantics by ensuring the invariance of the local-semantic representations of graphs that contain the same local structure.
- We conducted extensive experiments to demonstrate the effectiveness and efficiency of the proposed methods with multiple real-world and synthetic datasets.

2. Related works

2.1. Graph Representation Learning and Graph Generation

Surging development of deep-learning techniques, recent work on graph representation learning (Hamilton, 2020; Chen et al., 2020a; Hamilton et al., 2017), especially graph neural networks (GNN) (Wu et al., 2020; Zhou et al., 2020), is attracting considerable attention. Significant success has been achieved on developing various GNNs models to handle domain-specific graphs, such as traffic network (Yu & Gu, 2019; Zhang et al., 2019; Chen et al., 2019), social network (Zhong et al., 2020; Fan et al., 2019b), knowledge graph (Arora, 2020; Chen et al., 2020b; Tian et al., 2020) and materials structure (Park & Wolverton, 2020; Xie & Grossman, 2018; Lee & Asahi, 2021). Graph generation is one of the most important topics among the domain of graph representation learning. Due to the development of deep generative models, most GNN-based graph generation models borrow the framework of VAE (Kingma & Welling, 2013; Kipf & Welling, 2016; Higgins et al., 2016) or generative adversarial nets (GANs) (Goodfellow et al., 2014; Zhang et al., 2021; Zhou et al., 2019). For example,

GraphVAE learns the distribution of given graphs and generates small graphs under the framework of VAE (Simonovsky & Komodakis, 2018). JT-VAE was developed to generate molecular graphs under the VAE framework by first generating the tree-structured scaffold and then assembling them into molecules (Jin et al., 2018).

2.2. Disentangled Representation Learning

Disentangled representation learning has been attracting considerable attentions of the community, especially in the domain of computer vision (Chartsias et al., 2019; Tran et al., 2017; Zhao et al., 2019). The goal of disentangled representation learning is to separate underlying semantic factors accounting for the variation of the data in the learned representation. This disentangled representation has been shown to be resilient to the complex factors involved (Bengio et al., 2013), and can enhance the generalizability and improve robustness against adversarial attack (Guo et al., 2020a; Alemi et al., 2016). Intuitively, disentangled representation learning can achieve superior interpretability over regular graph representation learning tasks to better understand the graphs in various domains (Guo et al., 2020b). This motivates the surge of a few VAE-based approaches that modify the VAE objective by adding, removing or adjusting the weight of individual terms for deep graph generation tasks (Guo et al., 2020a; Chen et al., 2018; Kim & Mnih, 2018). Disentangled representation learning is important in modeling periodical graphs where the process requires to distinguish the repeatable patterns from the others.

2.3. Periodical Graph Learning

Periodic graph is the graph that consists of repetitive basic units in its structure, and can fit into the data structure in a number of domains, such as crystal structures in materials science (Blatov & Proserpio, 2010; Delgado-Friedrichs et al., 2017), polygon mesh in computer graphics (Foley et al., 1994) and motion planning in robotics (Fu et al., 2012). Several graph representation learning tasks have been conducted on this type of graph. For example, periodic graph-structured information in the airport network can be formatted into a periodic graph and a graph convolutional network-based (GCN-based) was developed for flight delay prediction (Cai et al., 2021). The multiple periodic spatial-temporal graphs of human mobility was employed learn the community structure based on a collective embedding model (Wang et al., 2018). In addition, graph generation model in periodic graphs can be categorized in to two scenarios: (1) domain specific-based models and (2) geometry-based models. For example, CDVAE borrows specific bonding preferences between different atoms and generates the periodic structure of materials in a diffusion process (Xie et al., 2021). Moreover,

(Ramsden et al., 2009) achieved geometric construction of periodic graphs by projecting two-dimensional hyperbolic tilings onto triply periodic minimal surfaces. They both need predefined rules to generate valid periodic graphs. Besides, the periodic graphs are usually large, the large time or space complexity of existing graph generative models limits the advance of periodic graph generation, motivating us to propose an end-to-end periodic graph generative model, PGD-VAE, that bears superior scalability on large periodic graphs.

3. Methodology

In this section, the problem formulation is first provided before moving on to derive the overall objective, following which the novel encoder of PGD-VAE that can respectively extract local and global information of the graph structure is introduced. Afterwards, the decoder that generates local and global structure, and the algorithm of the assembler are described.

3.1. Notations and Problem Definition

3.1.1. PERIODIC GRAPH

Define a periodic graph as $G = (\mathcal{V}, \mathcal{E}, A)$, where \mathcal{V} is the set of nodes and $\mathcal{E} \subseteq \mathcal{V} \times \mathcal{V}$ corresponds to the set of edges of the graph G . The repeated local structures can be defined as basic units of size n (i.e., number of nodes is n). Suppose the periodic graph G consists of m basic units as well as their connections, this means the node set $\mathcal{V} = \cup_{u=1}^m v_{i,u}$ is the union of nodes in all basic units, and $\mathcal{E} = \{\cup_{u=1}^m e_{ij,u}\} \cup \{\cup_{u \neq v}^m e_{ij,i \in u, j \in v}\}$ is the union of all edges within and across basic units of the graph. $A \in \mathbb{R}^{N \times N}$ corresponds to the adjacency matrix of the graph, in which $A_{ij} = 1$ if $e_{ij} \in \mathcal{E}$ and $A_{ij} = 0$ otherwise. In addition, we define three matrices: (1) $A^{(l)} \in \mathbb{R}^{n \times n}$ is the adjacency matrix of the basic unit of the graph; (2) $A^{(g)} \in \mathbb{R}^{m \times m}$ is the adjacency matrix denoting the pairwise relations among basic units; and (3) $A^{(n)} \in \mathbb{R}^{n \times n}$ is the incidence matrix regarding how the nodes in adjacent basic units are connected.

3.1.2. DENOTE A BY $A^{(l)}$, $A^{(g)}$, AND $A^{(n)}$

As the adjacency matrix A of the periodic graph contains a lot of repeated local structure, we want to use an alternative “deduplicated” way to represent A efficiently. This will be achieved by concisely representing A with a function of $A^{(l)}$, $A^{(g)}$, and $A^{(n)}$: $A = f(A^{(l)}, A^{(g)}, A^{(n)})$, which is detailed in the following and illustrated in the right part of Figure 2. First, define a binary block matrix $P \in \{0, 1\}^{nm \times m}$ s.t. $P \cdot P^T = J$, where J is the block diagonal matrix whose diagonal blocks are all 1’s. Then, $\hat{A}^{(g)}$, the augmentation of $A^{(g)}$ can be achieved as:

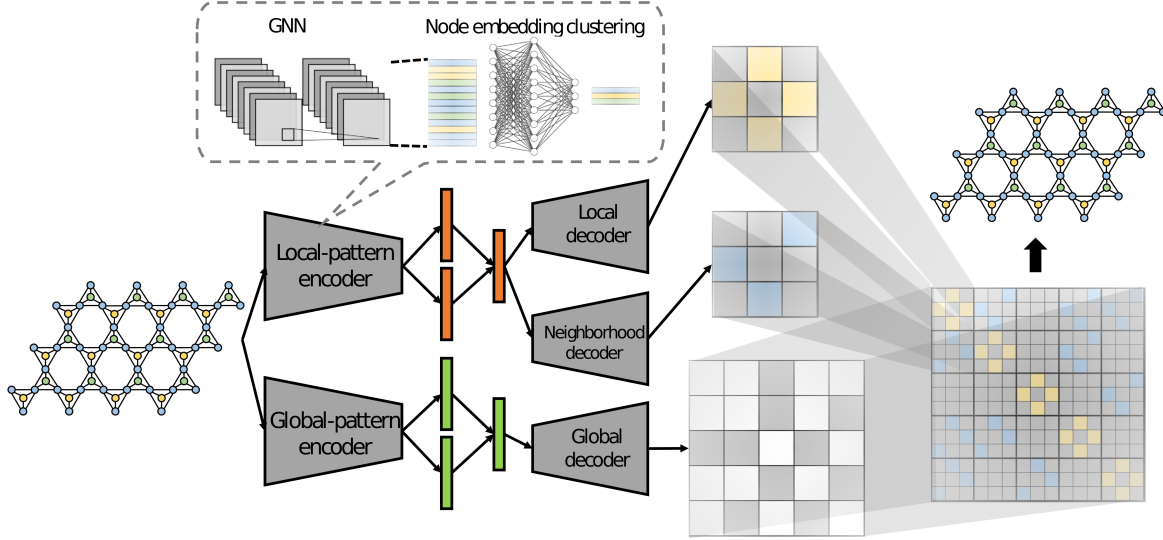


Figure 2. Overview of PGD-VAE. The graph representation z_l and z_g that respectively capture local and global semantics are learned by the local-pattern and global-pattern encoders, respectively. Then $A^{(l)}$, $A^{(n)}$ and $A^{(g)}$ are generated by local decoder, neighborhood decoder and global decoder, respectively. Finally, the generated graph is obtained by assembling $A^{(l)}$, $A^{(n)}$ and $A^{(g)}$.

$$\hat{A}^{(g)} = PA^{(g)}P^T. \quad (1)$$

Additionally, we define the matrix $Q \in \mathbb{R}^{nm \times n}$ as the concatenation of m identity matrices of size n . Then we can obtain $\hat{A}^{(l)}$, the repetition of $A^{(l)}$ along both dimensions by m :

$$\hat{A}^{(l)} = QA^{(l)}Q^T. \quad (2)$$

Similarly, we obtain $\hat{A}^{(n)}$ the repetition of $A^{(n)}$ via Q :

$$\hat{A}^{(n)} = QA^{(n)}Q^T. \quad (3)$$

Consequently, we can deterministically obtain A from $A^{(l)}$, $A^{(g)}$ and $A^{(n)}$ via the function f :

$$\begin{aligned} A &= f(A^{(l)}, A^{(g)}, A^{(n)}) \\ &= (M^{(n)} \odot QA^{(n)}Q^T + (M^{(n)} \odot QA^{(n)}Q^T)^T) \odot PA^{(g)}P^T \\ &\quad + M^{(l)} \odot QA^{(l)}Q^T \\ &= (M^{(n)} \odot \hat{A}^{(n)} + (M^{(n)} \odot \hat{A}^{(n)})^T) \odot \hat{A}^{(g)} \\ &\quad + M^{(l)} \odot \hat{A}^{(l)}, \end{aligned} \quad (4)$$

where $M^{(l)}$ and $M^{(n)}$ are two mask matrices. Specifically, the off-diagonal blocks of size n in $M^{(l)}$ are 0's while the diagonal blocks in $M^{(l)}$ are 1's. We also specify that the upper-triangular blocks of size n in $M^{(n)}$ are 1's and other blocks in $M^{(n)}$ are 0's. In the following, we may exchangeably use G and A to denote the whole graph since it is determined by its topology.

3.1.3. GENERATIVE MODELS OF PERIODIC GRAPHS

The goal of learning generative models for a periodic graph is to learn the conditional distribution $p(G|Z)$. Define

$Z = (z_l, z_g)$ as the learned graph representation based on the structure of the graphs. Specifically, z_l is designed to capture the local semantic factors that characterize the topological structure of basic units, while z_g is designed to represent the global semantics on how basic units are topologically connected.

3.2. Learning Deep Periodic Graph Generative models

We first introduce the variational inference of the generative model and learning objective. Then we introduce our local and global encoders, as well as the new periodic graph decoder.

3.2.1. PERIODIC GRAPH GENERATIVE MODEL INFERENCE

As discussed in the problem definition, we aim to learn the conditional distribution of G given $Z = (z_l, z_g)$. So we aim to maximize the marginal likelihood of the observed periodic graphs G in expectation over the distribution of the latent variables (z_l, z_g) . For a given periodic graph G , we define the prior distribution of the latent representation as $p(z_l, z_g)$ which is intractable to infer. As a result, we leverage variational inference, in which the posterior distribution is approximated by $q_\phi(z_l, z_g|G)$. Hence, another goal is to minimize the Kullback–Leibler (KL) divergence between the true prior and the approximated posterior distributions. To encourage the disentanglement of z_l and z_g , we introduce a constraint by matching the inferred posterior configurations of the latent factors $q_\phi(z_l, z_g|G)$ to the

prior distribution $p_\theta(z_l, z_g)$.

$$\begin{aligned} & \max_{\theta, \phi} \mathbb{E}_{G \sim D} [\mathbb{E}_{q_\phi(z_l, z_g | G)} \log p_\theta(G | z_l, z_g)] \\ & \text{s.t. } \mathbb{E}_{G \sim D} [KL(q_\phi(z_l, z_g | G) || p_\theta(z_l, z_g))] < I, \end{aligned} \quad (5)$$

where D refers to the observed graphs and I is a constant. Then, we can decompose the constraint term in Eq. 5 given the assumption that z_l and z_g are independent, leading to:

$$\begin{aligned} p_\theta(z_l, z_g) &= p_\theta(z_l)p_\theta(z_g) \\ q_\phi(z_l, z_g | G) &= q_\phi(z_l | G)q_\phi(z_g | G) \end{aligned} \quad (6)$$

Based on the problem formulation, G can be represented as $\{A^{(l)}, A^{(g)}, A^{(n)}\}$. Since z_l should capture and only capture the local patterns, thus $A^{(l)}$ and $A^{(n)}$ are dependent on z_l and conditional independent from each other given z_l , namely $A^{(l)} \perp A^{(n)} | z_l$. And z_g should capture and only capture the global patterns, we have

$$\begin{aligned} p_\theta(G | z_l, z_g) &= p_\theta(A^{(l)}, A^{(n)} | z_l)p_\theta(A^{(g)} | z_g) \\ &= p_\theta(A^{(l)} | z_l)p_\theta(A^{(n)} | z_l)p_\theta(A^{(g)} | z_g). \end{aligned} \quad (7)$$

Then, the objective function can be written as:

$$\begin{aligned} & \max_{\theta, \phi} \mathbb{E}_{G \sim D} [\mathbb{E}_{q_\phi(z_l, z_g | G)} \log p_\theta(A^{(l)} | z_l)p_\theta(A^{(n)} | z_l)p_\theta(A^{(g)} | z_g)] \\ & \text{s.t. } \mathbb{E}_{G \sim D} [KL(q_\phi(z_l | G) || p_\theta(z_l))] < I_l \\ & \mathbb{E}_{G \sim D} [KL(q_\phi(z_g | G) || p_\theta(z_g))] < I_g, \end{aligned} \quad (8)$$

where I_l and I_g are the information bottleneck to control the information captured by the latent vector z_l and z_g . Based on the objective we derived above, we propose a novel objective for PGD-VAE by modifying Eq. 8 that not only fulfills the optimization objective of the general VAE framework (Eq. 5), but also secure the disentanglement of local and global semantics of the graph. Specifically, we forced the z_l equal for graphs with the same basic unit (Eq. 3.2.2). At the meanwhile, we distinguish z_l 's of graphs with different basic units (Eq. 3.2.2).

$$\begin{aligned} & \max_{\theta, \phi} \mathbb{E}_{G \sim D} [\mathbb{E}_{q_\phi(z_l, z_g | G)} \log p_\theta(A^{(l)} | z_l)p_\theta(A^{(n)} | z_l)p_\theta(A^{(g)} | z_g)] \\ & \text{s.t. } \mathbb{E}_{G \sim D} [KL(q_\phi(z_l | G) || p_\theta(z_l))] < I_l \\ & \mathbb{E}_{G \sim D} [KL(q_\phi(z_g | G) || p_\theta(z_g))] < I_g \\ & z_{l,i}^{(j)} = z_{l,i}, j = 1, \dots, N_i, i = 1, \dots, N \\ & z_{l,s} \neq z_{l,t}, s = 1, \dots, N, t = 1, \dots, N, s \neq t \end{aligned} \quad (9)$$

where $z_{l,i}^{(j)}$ and $z_{g,i}^{(j)}$ are respectively the local and global representations of the j -th graph for the i -th basic unit. The derived objective function proposed for PGD-VAE (Eq. 3.2.2) can meet the objective in our problem formulation, as stated in Theorem 3.1. The proof of Theorem 3.1 is thus provided in Appendix A.

Theorem 3.1. *The proposed objective function in Eq. 3.2.2 guarantees that z_l and z_g have the following properties:*

1. z_l capture and only capture the local semantic of the graph;
2. z_g capture and only capture the global semantic of the graph.

3.2.2. LEARNING OBJECTIVES

To achieve the constraint and optimize the overall objective in Eq. 3.2.2, we transform the inequality constraint into tractable form. Given that I_l and I_g are constants, we rewrite the first two constraints of Eq. 3.2.2 using Lagrangian algorithm under KKT condition as:

$$\begin{aligned} L_{KL} &= -\beta_1 KL\{q_\phi(z_l | \mathbf{G}) || p_\theta(z_l)\} \\ & -\beta_2 KL\{q_\phi(z_g | \mathbf{G}) || p_\theta(z_g)\}, \end{aligned} \quad (10)$$

where \mathbf{G} represents a set of observed graphs, the Lagrangian multipliers β_1 and β_2 are regularization coefficients that constraints the capacity of latent information channels z_l and z_g , respectively, and put implicit pressure of independence on the learned posterior.

Additionally, the goal of the last two constraints of Eq. 3.2.2 is to enforce the graphs that contain the same repeat patterns (i.e., local information) share the same z_l and the graphs that contain different repeat patterns have different z_l . Thus, to both minimize the distances of z_l among the graphs with the same unit cell and maximize the distances of z_l among the graphs with different unit cells, we propose to minimize a contrastive loss L_{contra} as:

$$-\beta_3 \sum_{i=1}^N \sum_{j=1}^{N_i} \sum_{k=1}^{N_i} \log \frac{\exp\{\text{sim}(z_{l,i}^{(j)}, z_{l,i}^{(k)}) / \tau\}}{\sum_{s=1, s \neq i}^N \sum_{t=1}^{N_s} \exp\{\text{sim}(z_{l,i}^{(j)}, z_{l,s}^{(t)}) / \tau\}},$$

where τ is a predefined temperature parameter, and β_3 is the weights added on the contrastive loss to adjust the convergence of z_l in graphs with the same basic unit and the divergence in graphs with different basic units.

In summary, the final implemented loss function minimized includes three parts: (1) L_{recon} to minimize the reconstruction loss of the input and generated graphs; (2) L_{KL} to minimize the KL divergence of the posterior and its approximation; and (3) $L_{contrastive}$, the contrastive loss to force z_l equal for graphs with the same basic unit and different for those with different basic units:

$$\begin{aligned} & \max_{\theta, \phi} \mathbb{E}_{G \sim D} [\mathbb{E}_{q_\phi(z_l, z_g | G)} \log p_\theta(A^{(l)} | z_l)p_\theta(A^{(n)} | z_l)p_\theta(A^{(g)} | z_g)] \\ & + L_{KL} + L_{contra} \end{aligned} \quad (11)$$

3.3. Architecture of PGD-VAE

Based on the above periodic graph generative model and its learning objective, we are proposing our new Periodic Graph Disentangled VAE model (PGD-VAE). In general, PGD-VAE takes the whole adjacency matrix A as the input and can automatically identify $A^{(l)}$, $A^{(g)}$ and $A^{(n)}$ by model architecture and learning objective. Specifically, PGD-VAE contains a local-pattern encoder and a global-pattern encoder to disentangle the graph representation into local and global semantics, respectively. It also contains a local structure decoder, a global structure decoder, a neighborhood decoder together with an assembler to formalize the graph while ensuring the periodicity.

The overview of PGD-VAE is shown in Figure 2. The proposed framework has two encoders, each of which models one of the distributions $q_\theta(z_g|G)$ and $q_\theta(z_l|G)$; and three decoders to model $p_\theta(A^{(l)}|z_l)$, $p_\theta(A^{(n)}|z_l)$, and $p_\theta(A^{(g)}|z_g)$, respectively. Each type of representations is sampled using its own inferred mean and standard derivation. For example, the representation vectors z_l are sampled as $z_l = \mu_l + \sigma_l * \eta$, where η follows a standard normal distribution.

3.3.1. ENCODER

The encoder of PGD-VAE was designed to learn z_l and z_g such that z_l captures only the local semantics of the graph and z_g can capture only the global semantics of the graph. Thus, we propose a local-pattern encoder to encode the local information and a global-pattern encoder to encode the global information, as illustrated in Figure 2.

Local-pattern encoder We designed the encoder to learn an assignment matrix $A_{rep} \in \mathcal{R}^{C \times N}$ to identify representative nodes of the graph (Eq. 12) where C is predefined as the number of representative nodes to be assigned. This node embedding clustering module can enforce z_l to only capture the local information, namely excluding the global information (e.g., size of the graph) from z_l , because: 1) Each node embedding preserves local pattern since GIN embeds local information of nodes; b) Since node embedding of periodic graph is periodic, embedding of a node in a basic unit is the same as the corresponding node in another basic unit. By clustering all node embedding, each cluster preserves repetitive node embedding patterns across different local regions. In our setting, these representative nodes capture different embedding with each other. The column of A_{rep} corresponding to the node v can be calculated:

$$A_{rep,v} = \text{SOFTMAX}(\text{MLP}(h_v^{(K)}|v \in \mathcal{V})) \quad (12)$$

where $h_v^{(K)}$ is the embedding of node v at the last layer of Graph Isomorphism Network (GIN) (Xu et al., 2018). To preserve all information contained by the representative nodes, We concatenate all representative node embedding to obtain μ_l and σ_l :

$$\begin{aligned} \mu_l &= \text{MLP}(\text{CONCAT}(D_{A_{rep}}^{-1} \cdot A_{rep} \cdot h_v^{(K)}|v \in \mathcal{V})) \\ \sigma_l &= \text{MLP}(\text{CONCAT}(D_{A_{rep}}^{-1} \cdot A_{rep} \cdot h_v^{(K)}|v \in \mathcal{V})), \end{aligned} \quad (13)$$

where $D_{A_{rep}}$ has the degree of each cluster in its diagonal. z_l can then be sampled according the VAE framework: $z_l \sim \mathcal{N}(\mu_l, \sigma_l)$.

Global-pattern encoder To enforce the z_g capture all the global information, GIN is leveraged to generate node-level embedding of the graph. Additionally, PGD-VAE leverages sum aggregator as the graph-level readout (Eq. 14) to obtain the graph-level embedding z_g while achieving maximal discriminative power.

$$\begin{aligned} \mu_g &= \text{SUM}(\text{MLP}(h_v^{(K)}|v \in \mathcal{V})) \\ \sigma_g &= \text{SUM}(\text{MLP}(h_v^{(K)}|v \in \mathcal{V})) \end{aligned} \quad (14)$$

Table 1. Complexity of PGD-VAE and comparison models (n is the size of the basic unit, m is the size of the global pattern)

Model	Number of generation steps	Time complexity	Space complexity
VGAE	$O(1)$	$O((mn)^2)$	$O((nm)^2)$
GraphRNN	$O((nm)^2)$	$O((mn)^2)$	$O((nm)^2)$
GRAN	$O(nm)$	$O((mn)^2)$	$O((nm)^2)$
PGD-VAE	$O(1)$	$O(m^2 + n^2 + mn)$	$O(\max\{n^2, m^2\})$

The $h_v^{(K)}$ represents the embedding of node v obtained at the last layer of GIN. z_g can then be sample according to the VAE framework: $z_g \sim \mathcal{N}(\mu_g, \sigma_g)$.

3.3.2. DECODER

As shown in Figure 2, the decoder of contains four parts: (1) the local-structure decoder to generate $A^{(l)}$; (2) the global-structure decoder to generate $A^{(g)}$; (3) the neighborhood decoder f_n to generate $A^{(n)}$; and (4) an assembler $f : \{A^{(l)}, A^{(g)}, A^{(n)}\} \rightarrow A$ which generates A with Eq. (4). The local structure decoder takes the local-semantic representation z_l as the input to generate the structure of the basic unit. The global structure decoder takes the global-semantic representation z_g as the input to generate the global organization of basic units. Since how basic units are connected is regarded as the local structure of the graph, the neighborhood decoder takes the local-semantic representation z_l as the input to generate the connection between adjacent basic units. The assembler f is an closed-form function defined in Section 3.1 to assemble $A^{(l)}$, $A^{(g)}$ and $A^{(n)}$ into A , the adjacency matrix of generated graph \hat{G} :

$$A = f(A^{(l)}, A^{(g)}, A^{(n)}) \quad (15)$$

Here f_l , f_g , f_n are deterministic functions and are approximated by three multilayer perceptrons (MLP) in implementation.

3.4. Complexity Analysis

We theoretically evaluate the scalability of our model compared with comparison models in the number of generation steps, similar to the analysis in (Liao et al., 2019). Since the decoder of PGD-VAE follows an one-shot strategy using MLP, it requires $O(1)$ generation steps. Additionally, the space complexity of PGD-VAE is $O(\max\{n^2, m^2\})$, since the generated graph is determined by the basic units, the connection of adjacent basic units and the global pattern. The graph size can be calculated as mn . The number of generation steps of PGD-VAE is aligned with that of VGAE, but is lower than that of GraphVAE and GRAN. Nevertheless, PGD-VAE has the smallest space complexity. Regarding the time complexity, PGD-VAE model can achieve $O(m^2 + n^2 + mn)$ by using matrix replication and concatenation tricks in implementation, better than that of other comparison models. The number of generation steps, time complexity and the space complexity of PGD-VAE and comparison models are summarized in Table 1.

4. Experiments

This section reports the results of both quantitative and qualitative experiments that were performed to evaluate PGD-VAE with other comparison models. Two real-world datasets and one synthetic datasets of periodic graphs were employed in the experiments. All experiments were conducted on the 64-bit machine with an NVIDIA GPU, NVIDIA GeForce RTX 3090.

Table 2. PGD-VAE compared to state-of-the-art deep generative models on QMOF, MeshSeg and Synthetic datasets using KLD (KLD_cluster: KLD of clustering coefficient, KLD_dense: KLD of graph density, PGD-VAE-1: PGD-VAE without regularization, PGD-VAE-2: PGD-VAE replacing GIN with GCN in encoder, PGD-VAE-3: PGD-VAE with single MLP as decoder)

Method	QMOF		MeshSeq		Synthetic	
	KLD_cluster	KLD_dense	KLD_cluster	KLD_dense	KLD_cluster	KLD_dense
VGAE(Kipf & Welling, 2016)	1.7267	1.5168	0.9723	0.9642	4.6196	1.4222
GraphRNN(You et al., 2018)	3.1055	5.0048	1.4316	1.0271	6.4719	3.6064
GRAN(Liao et al., 2019)	3.3107	2.7208	1.2466	0.8879	5.7501	2.3020
PGD-VAE-1	1.0193	1.0250	0.4630	0.4921	3.2672	0.8399
PGD-VAE-2	0.8508	0.9332	0.4539	0.4862	4.1596	2.7684
PGD-VAE-3	0.9597	1.0224	0.5496	0.5099	3.3850	0.9366
PGD-VAE	1.0164	1.0512	0.3977	0.4535	3.1863	0.6824

Table 3. PGD-VAE compared to state-of-the-art deep generative models on QMOF, MeshSeg and Synthetic datasets according to uniqueness and novelty (PGD-VAE-1: PGD-VAE without regularization, PGD-VAE-2: PGD-VAE replacing GIN with GCN in encoder, PGD-VAE-3: PGD-VAE with single MLP as decoder)

Method	QMOF		MeshSeq		Synthetic	
	Uniqueness	Novelty	Uniqueness	Novelty	Uniqueness	Novelty
VGAE(Kipf & Welling, 2016)	100%	100%	100%	100%	100%	100%
GraphRNN(You et al., 2018)	23.34%	100%	71.39%	100%	26.76%	100%
GRAN(Liao et al., 2019)	8.00%	100%	15.33%	100%	18.67%	100%
PGD-VAE-1	100%	100%	100%	100%	100%	100%
PGD-VAE-2	100%	100%	100%	100%	100%	100%
PGD-VAE-3	100%	100%	100%	100%	100%	100%
PGD-VAE	100%	100%	100%	100%	100%	100%

4.1. Data

Two real-world datasets and one synthetic dataset were employed to evaluate the performance of PGD-VAE and other comparison models. All the comparison and our proposed methods only take the whole adjacency matrix A . The information of $A^{(l)}$, $A^{(g)}$, and $A^{(n)}$ are hidden from all the methods. 1) **QMOF dataset** is a publicaly available database of computed quantum-chemical properties and molecular structures (Rosen et al., 2021). We trimmed the QMOF dataset by only selecting metal-organic frameworks (MOFs) consisting of unit cells with the size less than 20 as the basic unit (i.e., $A^{(l)}$). $A^{(g)}$ and $A^{(n)}$ can be automatically determined by Atomic Simulation Environment (ASE) (Larsen et al., 2017). Finally, the whole adjacency matrix A was synthesized by combining the generated $A^{(l)}$, $A^{(g)}$ and $A^{(n)}$. 2) **MeshSeg dataset** contains 380 meshes for quantitative analysis of how people decompose objects into parts and for comparison of mesh segmentation algorithms (Chen et al., 2009). We trimmed the dataset by selecting meshes whose size is less than 1000 and making 10 replicates for each mesh. The whole adjacency matrix A was directly obtained from the graphs in this dataset. 3) **Synthetic dataset**. Three synthetic datasets were generated based on three different basic units (i.e., $A^{(l)}$), triangle, grid and hexagon, respectively. For each of the above basic unit types, different number of basic units were used to compose the whole graph (i.e., represented by the whole adjacency matrix A) via Equation (4), with self-designed $A^{(g)}$ and $A^{(n)}$. All adjacency matrices were padded into a fixed size with zeroes in implementation. The statistics of the three dataset has been summarized in Table 4 and more details can be found in Appendix B.

Table 4. Overview of datasets in experiments ($|G|$ is the total number periodic graphs in the dataset; $|\mathcal{V}|_{avg}$ is the average graphs size of the dataset; $|\mathcal{E}|_{avg}$ is the average edges of the graph in the dataset; $|\mathbf{U}|$ is the types of basic units in the dataset; $|U|_{avg}$ is the average size of basic units in the dataset)

Property	QMOF	MeshSeg	Synthetic
$ G $	3,780	300	46,500
$ \mathcal{V} _{avg}$	151.42	662.13	71.09
$ \mathcal{E} _{avg}$	1004.13	1747.24	107.34
$ \mathbf{U} $	14	1	3
$ U _{avg}$	18.93	3	4.33

4.2. Comparison Models

Three state-of-the-art deep generative models were employed as comparison models to compare with PGD-VAE¹: (1) VGAE, a simple VAE-based graph generative model (Kipf & Welling, 2016) by learning the graph-level representation and employing MLP to generate the adjacent matrix; *GraphRNN*, a deep autoregressive model that accounts for non-local dependencies of edges by decomposing graph generation process into a sequence of node and edge conformations (You et al., 2018); and *GRAN*, a deep autoregressive model for graph generation (Liao et al., 2019) which generates block of nodes and associated edges at a time, and captures the auto-regressive conditioning between the already-generated and to-be-generated pieces of the graph using GNNs with attention. Both our method PGD-VAE and all comparison

¹Some graph generative models, such as GraphVAE that employs $O(n^4)$ on its max-pooling matching algorithm, are not included in the comparison due to its poor scalability to large graphs, which is common in QMOF and MeshSeg datasets.

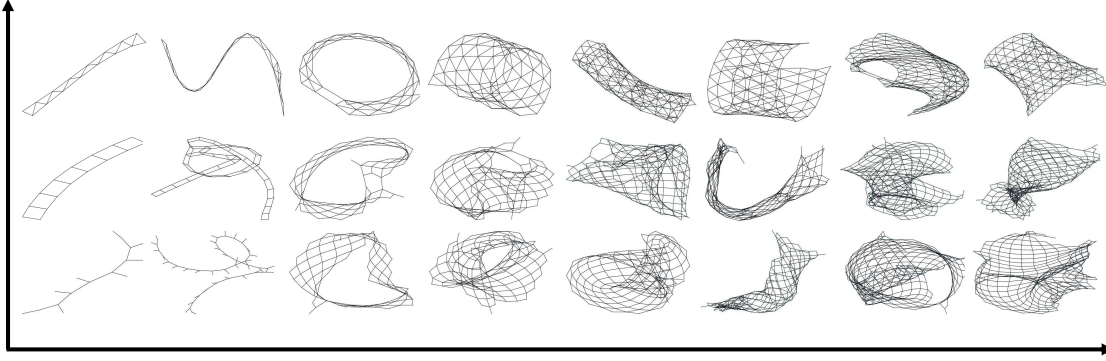


Figure 3. Visualizing the variations of generated periodical graphs regarding local and global semantics

methods only take the whole adjacency matrix A as input, without extra information on $A^{(l)}$, $A^{(g)}$, or $A^{(n)}$.

In addition, three ablation study are conducted by evaluating three variants of PGD-VAE: (1) PGD-VAE without regularization term; (2) PGD-VAE replacing GIN with GCN in the encoder; and (3) PGD-VAE with a single MLP as decoder.

4.3. Evaluating the Generated Graphs

Quantitative evaluation. To quantitatively evaluate generation performance of PGD-VAE and comparison models, we compute the KL Divergence (KLD) between generated and ground-truth graphs to measure the similarity of their distributions regarding: (1) average clustering coefficient and (2) density of graphs (Guo et al., 2021). Moreover, we adopt uniqueness and novelty to evaluate generation graphs. Ideally the generated set of graphs should be diverse and similar but not identity. Thus, the uniqueness measures the diversity of generated graphs. The novelty determines whether the model has generated unseen graphs by measuring the proportion of generated graphs that are not in the set of training graphs. The KLD-based results of PGD-VAE compared with comparison models were calculated and shown in Table 2. The results show that, even provided numerous periodic graphs with different sizes in the datasets, PGD-VAE and its variants can still learn the distribution of graphs with the closer match with testing data. Specifically, PGD-VAE achieves KLD smaller than comparison models by 0.8191 for clustering coefficient and 0.5062 for graph density on average regarding MeshSeq dataset, and 2.4275 for clustering coefficient as well as 1.7611 for graph density on average on Synthetic dataset. Interestingly, on QM0F dataset, PGD-VAE that replaces GIN with GCN achieve KLD of 0.8508 regarding clustering coefficient and 0.9332 regarding graph density, outperforming but close to other evaluated models, which is likely due to the fact that the basic unit of MOF is usually large and needs more layers of GNN in the encoder to capture the local information of the graph. However, here PGD-VAE and its variants use three-layer GIN/GCN in the encoder, which might limit the significance of the superior discriminative power of GIN over GCN. Moreover, the number of representative nodes in the graph is predefined as 5 prior to the node clustering module in the encoder of PGD-VAE. Since the large basic unit in MOF might have more than 5 representative nodes, which cannot be covered by the node clustering module leading to the loss of information.

The results regarding the uniqueness and novelty of generated graphs based on comparison models, PGD-VAE and its variants have been summarized in Table 3. PGD-VAE and all its

variants, together with VGAE achieves better performance than GraphRNN and GRAN, as they tend to generate unique graphs, which is desired for domains such as materials design and object synthesis. All evaluated models can generate novel graphs, as shown in Table 3.

Qualitative evaluation for disentanglement To validate the disentanglement of local and global semantics in the graph representation, we qualitatively explore whether PGD-VAE can uncover and disentangle these two latent factors. To this end, we continuously changing the value of z_l or z_g while keeping another latent vector fixed and simultaneously visualizing the change of generated graphs. Figure 3 shows the variation of generated graphs when traversing two latent factors z_l and z_g .

4.4. Evaluating Scalability

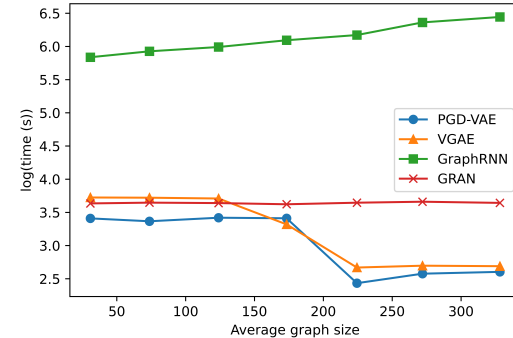


Figure 4. Scalability evaluation by running 10 epochs of PGD-VAE and comparison models

We also conducted experiments to evaluate the time complexity of PGD-VAE and comparison models, as shows in Figure 4. In the experiments, we recorded and logarithmized the time (s) to run 10 epochs on graphs in stratified synthetic dataset according to average graph size with PGD-VAE and comparison models. Aligned with the theoretical analysis above, GraphVAE consumes the most of time compare with other models. Given the synthetic dataset, GRAN spends slightly more time than PGD-VAE and VGAE, while PGD-VAE and VGAE are less computational intensive and have comparable performance.

5. Conclusion

In this paper we propose PGD-VAE, a novel VAE-based deep generative model for periodic graphs that can automatically learn, disentangle, and generate local and global patterns. Our method can guarantee the periodicity of generated graphs and outperforms existing graph generative models in periodic graph generation, both quantitatively and qualitatively. The paper does not have concern regarding the societal implications. In the future, we attempt to introduce more information, including the node and edge features, into the model to advance domains such as materials design and object synthesis.

References

Alemi, A. A., Fischer, I., Dillon, J. V., and Murphy, K. Deep variational information bottleneck. *arXiv preprint arXiv:1612.00410*, 2016.

Arora, S. A survey on graph neural networks for knowledge graph completion. *arXiv preprint arXiv:2007.12374*, 2020.

Bengio, Y., Courville, A., and Vincent, P. Representation learning: A review and new perspectives. *IEEE transactions on pattern analysis and machine intelligence*, 35(8):1798–1828, 2013.

Blatov, V. A. and Proserpio, D. M. Periodic-graph approaches in crystal structure prediction. 2010.

Bushlanov, P. V., Blatov, V. A., and Oganov, A. R. Topology-based crystal structure generator. *Computer Physics Communications*, 236:1–7, 2019.

Cai, K., Li, Y., Fang, Y.-P., and Zhu, Y. A deep learning approach for flight delay prediction through time-evolving graphs. *IEEE Transactions on Intelligent Transportation Systems*, 2021.

Chartsias, A., Joyce, T., Papanastasiou, G., Semple, S., Williams, M., Newby, D. E., Dharmakumar, R., and Tsaftaris, S. A. Disentangled representation learning in cardiac image analysis. *Medical image analysis*, 58:101535, 2019.

Chen, C., Li, K., Teo, S. G., Zou, X., Wang, K., Wang, J., and Zeng, Z. Gated residual recurrent graph neural networks for traffic prediction. In *Proceedings of the AAAI conference on artificial intelligence*, volume 33, pp. 485–492, 2019.

Chen, F., Wang, Y.-C., Wang, B., and Kuo, C.-C. J. Graph representation learning: A survey. *APSIPA Transactions on Signal and Information Processing*, 9, 2020a.

Chen, R. T., Li, X., Grosse, R., and Duvenaud, D. Isolating sources of disentanglement in variational autoencoders. *arXiv preprint arXiv:1802.04942*, 2018.

Chen, X., Golovinskiy, A., and Funkhouser, T. A benchmark for 3D mesh segmentation. *ACM Transactions on Graphics (Proc. SIGGRAPH)*, 28(3), August 2009.

Chen, Y., Wu, L., and Zaki, M. J. Toward subgraph guided knowledge graph question generation with graph neural networks. *arXiv preprint arXiv:2004.06015*, 2020b.

Delgado-Friedrichs, O., Hyde, S. T., O’Keeffe, M., and Yaghi, O. M. Crystal structures as periodic graphs: the topological genome and graph databases. *Structural Chemistry*, 28(1):39–44, 2017.

Fan, F., Yuan, H., Feng, Y., Liu, F., Zhang, L., Liu, X., Zhu, X., An, W., Rohani, S., and Lu, J. Molecular simulation approaches for the prediction of unknown crystal structures and solubilities of (r)-and (r, s)-crizotinib in organic solvents. *Crystal Growth and Design*, 19(10):5882–5895, 2019a.

Fan, W., Ma, Y., Li, Q., He, Y., Zhao, E., Tang, J., and Yin, D. Graph neural networks for social recommendation. In *The World Wide Web Conference*, pp. 417–426, 2019b.

Foley, J. D., Van Dam, A., Feiner, S. K., Hughes, J. F., and Phillips, R. L. *Introduction to computer graphics*, volume 55. Addison-Wesley Reading, 1994.

Friedrichs, O. D., Dress, A. W., Huson, D. H., Klinowski, J., and Mackay, A. L. Systematic enumeration of crystalline networks. *Nature*, 400(6745):644–647, 1999.

Fu, N., Hashikura, A., and Imai, H. Geometrical treatment of periodic graphs with coordinate system using axis-fiber and an application to a motion planning. In *2012 Ninth International Symposium on Voronoi Diagrams in Science and Engineering*, pp. 115–121. IEEE, 2012.

Goodfellow, I. J., Pouget-Abadie, J., Mirza, M., Xu, B., Warde-Farley, D., Ozair, S., Courville, A., and Bengio, Y. Generative adversarial networks, 2014.

Guo, X. and Zhao, L. A systematic survey on deep generative models for graph generation. *arXiv preprint arXiv:2007.06686*, 2020.

Guo, X., Zhao, L., Qin, Z., Wu, L., Shehu, A., and Ye, Y. Interpretable deep graph generation with node-edge co-disentanglement. In *Proceedings of the 26th ACM SIGKDD international conference on knowledge discovery & data mining*, pp. 1697–1707, 2020a.

Guo, X., Zhao, L., Qin, Z., Wu, L., Shehu, A., and Ye, Y. Node-edge co-disentangled representation learning for attributed graph generation. In *International Conference on Knowledge Discovery and Data Mining (SIGKDD)*, 2020b.

Guo, X., Du, Y., and Zhao, L. Deep generative models for spatial networks. In *Proceedings of the 27th ACM SIGKDD Conference on Knowledge Discovery & Data Mining*, pp. 505–515, 2021.

Hamilton, W. L. Graph representation learning. *Synthesis Lectures on Artificial Intelligence and Machine Learning*, 14(3): 1–159, 2020.

Hamilton, W. L., Ying, R., and Leskovec, J. Representation learning on graphs: Methods and applications. *arXiv preprint arXiv:1709.05584*, 2017.

Higgins, I., Matthey, L., Pal, A., Burgess, C., Glorot, X., Botvinick, M., Mohamed, S., and Lerchner, A. beta-vae: Learning basic visual concepts with a constrained variational framework. *arXiv preprint*, 2016.

Jin, W., Barzilay, R., and Jaakkola, T. Junction tree variational autoencoder for molecular graph generation. In *International conference on machine learning*, pp. 2323–2332. PMLR, 2018.

Kim, H. and Mnih, A. Disentangling by factorising. In *International Conference on Machine Learning*, pp. 2649–2658. PMLR, 2018.

Kingma, D. P. and Welling, M. Auto-encoding variational bayes. *arXiv preprint arXiv:1312.6114*, 2013.

Kipf, T. N. and Welling, M. Variational graph auto-encoders. *arXiv preprint arXiv:1611.07308*, 2016.

Korn, P. and Linardakis, L. A conservative discretization of the shallow-water equations on triangular grids. *Journal of Computational Physics*, 375:871–900, 2018.

Larsen, A. H., Mortensen, J. J., Blomqvist, J., Castelli, I. E., Christensen, R., Dułak, M., Friis, J., Groves, M. N., Hammer, B., Hargus, C., et al. The atomic simulation environment—a python library for working with atoms. *Journal of Physics: Condensed Matter*, 29(27):273002, 2017.

Le Bail, A. Inorganic structure prediction with grinsp. *Journal of applied crystallography*, 38(2):389–395, 2005.

Lee, J. and Asahi, R. Transfer learning for materials informatics using crystal graph convolutional neural network. *Computational Materials Science*, 190:110314, 2021.

Liao, R., Li, Y., Song, Y., Wang, S., Nash, C., Hamilton, W. L., Duvenaud, D., Urtasun, R., and Zemel, R. S. Efficient graph generation with graph recurrent attention networks. *arXiv preprint arXiv:1910.00760*, 2019.

Park, C. W. and Wolverton, C. Developing an improved crystal graph convolutional neural network framework for accelerated materials discovery. *Physical Review Materials*, 4(6):063801, 2020.

Ramsden, S. , Robins, V., and Hyde, S. Three-dimensional euclidean nets from two-dimensional hyperbolic tilings: kaleidoscopic examples. *Acta Crystallographica Section A: Foundations of Crystallography*, 65(2):81–108, 2009.

Ranzato, M., Susskind, J., Mnih, V., and Hinton, G. On deep generative models with applications to recognition. In *CVPR 2011*, pp. 2857–2864. IEEE, 2011.

Rosen, A. S., Iyer, S. M., Ray, D., Yao, Z., Aspuru-Guzik, A., Gagliardi, L., Notestein, J. M., and Snurr, R. Q. Machine learning the quantum-chemical properties of metal–organic frameworks for accelerated materials discovery. *Matter*, 4(5):1578–1597, 2021.

Simonovsky, M. and Komodakis, N. Graphvae: Towards generation of small graphs using variational autoencoders. In *International conference on artificial neural networks*, pp. 412–422. Springer, 2018.

Tabero, P., Frackowiak, A., Filipek, E., Dbrowska, G., Homonnay, Z., and Szilagyi, P. Synthesis, thermal stability and unknown properties of fe1-xalxvo4 solid solution. *Ceramics International*, 44(15):17759–17766, 2018.

Tian, A., Zhang, C., Rang, M., Yang, X., and Zhan, Z. Ra-gcn: Relational aggregation graph convolutional network for knowledge graph completion. In *Proceedings of the 2020 12th International Conference on Machine Learning and Computing*, pp. 580–586, 2020.

Tran, L., Yin, X., and Liu, X. Disentangled representation learning gan for pose-invariant face recognition. In *Proceedings of the IEEE conference on computer vision and pattern recognition*, pp. 1415–1424, 2017.

Treacy, M., Rivin, I., Balkovsky, E., Randall, K., and Foster, M. Enumeration of periodic tetrahedral frameworks. ii. polynodal graphs. *Microporous and Mesoporous Materials*, 74(1-3):121–132, 2004.

Wang, P., Fu, Y., Zhang, J., Li, X., and Lin, D. Learning urban community structures: A collective embedding perspective with periodic spatial-temporal mobility graphs. *ACM Transactions on Intelligent Systems and Technology (TIST)*, 9(6):1–28, 2018.

Wu, Z., Pan, S., Chen, F., Long, G., Zhang, C., and Philip, S. Y. A comprehensive survey on graph neural networks. *IEEE transactions on neural networks and learning systems*, 32(1):4–24, 2020.

Xie, T. and Grossman, J. C. Crystal graph convolutional neural networks for an accurate and interpretable prediction of material properties. *Physical review letters*, 120(14):145301, 2018.

Xie, T., Fu, X., Ganea, O.-E., Barzilay, R., and Jaakkola, T. Crystal diffusion variational autoencoder for periodic material generation, 2021.

Xu, K., Hu, W., Leskovec, J., and Jegelka, S. How powerful are graph neural networks? *arXiv preprint arXiv:1810.00826*, 2018.

You, J., Ying, R., Ren, X., Hamilton, W., and Leskovec, J. Graphrnn: Generating realistic graphs with deep autoregressive models. In *International conference on machine learning*, pp. 5708–5717. PMLR, 2018.

Yu, J. J. Q. and Gu, J. Real-time traffic speed estimation with graph convolutional generative autoencoder. *IEEE Transactions on Intelligent Transportation Systems*, 20(10):3940–3951, 2019.

Zhang, L., Zhao, L., Qin, S., Pfoser, D., and Ling, C. Tg-gan: Continuous-time temporal graph deep generative models with time-validity constraints. In *Proceedings of the Web Conference 2021*, pp. 2104–2116, 2021.

Zhang, Y., Wang, S., Chen, B., and Cao, J. Grgan: Generative adversarial nets with graph cnn for network-scale traffic prediction. In *2019 International Joint Conference on Neural Networks (IJCNN)*, pp. 1–8. IEEE, 2019.

Zhao, J., Cheng, Y., Cheng, Y., Yang, Y., Zhao, F., Li, J., Liu, H., Yan, S., and Feng, J. Look across elapse: Disentangled representation learning and photorealistic cross-age face synthesis for age-invariant face recognition. In *Proceedings of the AAAI conference on artificial intelligence*, volume 33, pp. 9251–9258, 2019.

Zhong, T., Wang, T., Wang, J., Wu, J., and Zhou, F. Multiple-aspect attentional graph neural networks for online social network user localization. *IEEE Access*, 8:95223–95234, 2020.

Zhou, D., Zheng, L., Xu, J., and He, J. Misc-gan: A multi-scale generative model for graphs. *Frontiers in big Data*, 2:3, 2019.

Zhou, J., Cui, G., Hu, S., Zhang, Z., Yang, C., Liu, Z., Wang, L., Li, C., and Sun, M. Graph neural networks: A review of methods and applications. *AI Open*, 1:57–81, 2020.

A. Proof of Theorem 1

Proof. We assume that the periodic graph is simulated from two latent factors as $G = \text{Sim}(F_l, F_g)$, where F_l is the factor that is related to the local information, such as the structure of the repeating pattern and how repeating patterns are linked to each other. F_g is defined as the factor of the global information, including how many repeating patterns the graph contains and their spatial arrangements. The goal is to prove that z_l captures and only captures the information of F_l , and z_g captures and only captures the information of F_g . Thus, based on the information theory, we need to prove $I(z_l, F_l) = H(F_l)$, $I(z_l, F_g) = 0$, $I(z_g, F_g) = H(F_g)$, and $I(z_g, F_l) = 0$. Here $I(a, b)$ refers to the mutual information between a and b , and $H(*)$ refers to the information entropy of an element.

Based on the reconstruction error, after the model is well optimized, we can have all the latent variables to reconstruct the whole graph G . We also have $z_l \perp z_g$ and $F_l \perp F_g$ consider that the z_l and z_g are disentangled. Thus we have $I(z_l, F_l) + I(z_g, F_l) = H(F_l)$ and $I(z_l, F_g) + I(z_g, F_g) = H(F_g)$. Then we combine them to get

$$I(z_l, F_l) + I(z_l, F_g) + I(z_g, F_l) + I(z_g, F_g) = H(F_l) + H(F_g). \quad (16)$$

(1) First, we prove that $I(z_l, F_g) = 0$. Suppose we have two graphs (G_1, G_2) with the same repeat pattern (i.e. $F_{l,1} = F_{l,2}$ and different global information (i.e. $F_{g,1} \neq F_{g,2}$). Regarding the latent variables, We have $I(z_{l,1}, F_{l,1}) + I(z_{l,1}, F_{g,1}) = H(z_{l,1})$ and $I(z_{l,2}, F_{l,2}) + I(z_{l,2}, F_{g,2}) = H(z_{l,2})$. Based on the condition (i.e. subject to) of the loss function, we enforce $z_{l,1} = z_{l,2}$. Thus, we have

$$I(z_{l,1}, F_{l,1}) + I(z_{l,1}, F_{g,1}) = I(z_{l,2}, F_{l,2}) + I(z_{l,2}, F_{g,2}). \quad (17)$$

Since $F_{l,1} = F_{l,2}$, we have $I(z_{l,1}, F_{l,1}) = I(z_{l,2}, F_{l,2})$. Then we should have $I(z_{l,1}, F_{g,1}) = I(z_{l,2}, F_{g,2})$. However, since $F_{g,1} \neq F_{g,2}$, the only situation to meet the requirement is $I(z_{l,1}, F_{g,1}) = I(z_{l,2}, F_{g,2}) = 0$. Thus, to generalize, for any graph, we have $I(z_l, F_g) = 0$.

(2) Second, we prove that $I(z_g, F_g) = H(F_g)$. Based on the conclusion that $I(z_l, F_g) = 0$ from last step, and the conclusion from the second paragraph that $I(z_l, F_g) + I(z_g, F_g) = H(F_g)$, we can get $I(z_g, F_g) = H(F_g)$.

(3) Third, we prove that $I(z_g, F_l) = 0$. We can rewrite the loss function as:

$$\begin{aligned} \max_{\theta, \phi} I(z_l, G) + I(z_g, G) \\ I(G, z_l) \leq I_1 \\ I(G, z_g) \leq I_2 \end{aligned} \quad (18)$$

The detail of this derivation is provided in the work proposed by (Guo et al., 2021). When I_2 is defined as $I_2 \leq H(F_g)$, we can have $I(G, z_g) \leq H(F_g)$. Since $G = \text{Sim}(F_l, F_g)$, it can be written as

$$I(z_g, F_l) + I(z_g, F_g) \leq H(F_g). \quad (19)$$

From the second step, we already have $I(z_g, F_g) = H(F_g)$. Thus, we have $I(z_g, F_l) = 0$.

(4) Forth, we prove $I(z_l, F_l) = H(F_l)$. Based on the conclusion from the first three steps, we have $I(z_l, F_g) = 0$, $I(z_g, F_g) = H(F_g)$, and $I(z_g, F_l) = 0$. When we combine these three three equations with Eq.(16), we can have $I(z_l, F_l) = H(F_l)$.

Given the above four steps, we have finally proved the four equations $I(z_l, F_l) = H(F_l)$, $I(z_l, F_g) = 0$, $I(z_g, F_g) = H(F_g)$, and $I(z_g, F_l) = 0$, which indicate that the latent vector z_l capture and only capture local patterns and the latent vector z_g capture and only capture global patterns.

□

B. Dataset

Two real-world datasets and one synthetic dataset were employed to evaluate the performance of PGD-VAE and other comparison models.

QMOF dataset The Quantum MOF (QMOF) Database is a publicaly available database of computed quantum-chemical properties and molecular structures of 21,059 experimentally synthesized metal-organic frameworks (MOF) (Rosen et al., 2021). We trimmed the QMOF dataset by only selecting MOFs consisting of unit cells with the size less than 20. Then we only selected MOFs that have less than 27 unit cells. In total 3,780 MOFs were selected for the experiment. The statistics of the QMOF dataset was summarized in Table 4.

MeshSeg dataset The 3D Mesh Segmentation project contains 380 meshes for quantitative analysis of how people decompose objects into parts and for comparison of mesh segmentation algorithms (Chen et al., 2009). Meshes in MeshSeg dataset can be formed into graphs of triangle grids. We trimmed the dataset by selecting meshes whose size is less than 1000 and making 10 replicates for each mesh. Finally, 300 graphs were recruited for our experiment. The statistics of MeshSeg dataset has been summarized in Table 4.

Synthetic dataset The synthetic dataset contains three types of basic units: triangle, grid and hexagon. The statistics of the synthetic dataset has been summarized in Table 4. We augmented each basic unit to contain more basic units and finally we obtained 15,500 graphs for each local pattern. The statistics of synthetic dataset has been summarized in Table 4.